

New Strategy for Surface Functionalization of Periodic Mesoporous Silica Based on meso-HSiO_{1.5}

Zhuoying Xie,^{*,†,‡} Ling Bai,[†] Suwen Huang,[†] Cun Zhu,[†] Yuanjin Zhao,[†] and Zhong-Ze Gu^{*,†,‡}

[†]State Key Laboratory of Bioelectronics, School of Biological Science and Medical Engineering, Southeast University, Nanjing 210096, China

[‡]Laboratory of Environment and Biosafety, Research Institute of Southeast University in Suzhou, Suzhou 215123, China

S Supporting Information

ABSTRACT: Organic functionalization of periodic mesoporous silicas (PMSs) offers a way to improve their excellent properties and wide applications owing to their structural superiority. In this study, a new strategy for organic functionalization of PMSs is demonstrated by hydrosilylation of the recently discovered “impossible” periodic mesoporous hydridosilica, meso-HSiO_{1.5}. This method overcomes the disadvantages of present pathways for organic functionalization of PMSs with organosilica. Moreover, compared to the traditional functionalization on the surface of porous silicon by hydrosilylation, the template-synthesized meso-HSiO_{1.5} is more flexible to access functional-groups-loaded PMSs with adjustable microstructures. The new method and materials will have wider applications based on both the structure and surface superiorities.

Since the first report of templated synthesis of MCM-41 by scientists from the Mobil Oil Company in 1992, the synthesis, characterization, and application of periodic mesoporous silicas (PMSs) has become a hot research topic.¹ However, the application of pure PMSs is limited due to their simplex pore surface properties. Functionalizing PMSs with organic groups is an effective strategy to solve this problem. By introducing organic functional groups in the nanopores, the surface and interfacial properties of PMSs, including the hydrophilicity, hydrophobicity, linked guest molecules, and chemical activity,² could be adjusted to improve their properties and applications owing to the structural superiority.³

Incorporation of organic functionalities usually can be achieved via three pathways.⁴ The most common one is “grafting”, which attaches organic components onto the pore surface of pure PMSs by the reaction of organosilanes subsequent to the synthesis.⁵ This method of modification can well retain the mesostructure of the starting PMSs, but the mesopores are often narrowed or even completely blocked.⁶ To avoid blocking the pores requires rigorous grafting conditions; usually, the graft should be processed in anhydrous solvents.⁷ The second method is “co-condensation” of tetraalkoxysilanes (R'O)₄Si with terminal trialkoxyorganosilanes of the type (R'O)₃SiR in the presence of structure-directing agents, where R is a terminal organic group and R' is H or an alkyl group. Since the organic groups exist in the silane species directly, the blocking of pores can be avoided, and the dispersion of organic

groups is more uniform. But the pore ordering declines with increasing concentration of organic groups.⁸ In this context, a prevailing opinion in the field of PMSs is that the stability of these solids with respect to densification is predicated upon the existence of a robust, four-connected network of tetrahedral SiO₄ building blocks and that a maximum of 25% three-connected RSiO₃ units can be tolerated before the open framework collapses.⁹ As a result, the modified functional groups are very limited, usually <10%. The third pathway is creation of “periodic mesoporous organosilicas (PMOs)” by hydrolysis and condensation reactions of bridged organosilica precursors of the type (R'O)₃Si–R–Si(OR')₃.¹⁰ In PMOs, the organic units are homogeneously distributed in the pore walls and do not block the pore channels or occupy the pore volume. Particularly, incorporation of flexible organic groups through two covalent bonds can improve the mechanical strength, adjust the surface hydrophilicity/hydrophobicity, and provide new active centers. However, the PMOs also have some significant disadvantages. For the soft organic groups, especially the long-chain molecules, it is difficult to obtain ordered mesoporous structures. Moreover, the activity of organic groups is low because they are embedded in the pore walls of PMOs. Besides, the syntheses of some complex bridged organosilica precursors, as well as the control of morphology and structure of the PMOs, are difficult.¹¹ Hence, a new strategy is needed to resolve the disadvantages of the present pathways for organic functionalization of PMSs.

In this context, the recently discovered “impossible” periodic mesoporous hydridosilica, meso-HSiO_{1.5}, uniquely provided active sites of Si–H covering the pore surfaces and throughout the pore walls.¹² It could serve as a novel solid-state reactive host material within which one can perform novel chemistry and create numerous new materials. For example, Dag et al. have synthesized photoluminescent molecular Ag nanoclusters by reducing Ag⁺ ions via Si–H groups located within the pore walls of meso-HSiO_{1.5}.¹³ For the material, the Si–H bonds also offer new opportunities for surface functionalization with organic groups by terminal unsaturated compound through hydrosilylation.¹⁴ In the investigation described herein, we demonstrate that a new strategy for organic functionalization of PMSs can be realized by hydrosilylation of meso-HSiO_{1.5}, which overcomes the disadvantages of present pathways for organic functionalization of PMSs. First, compared to the

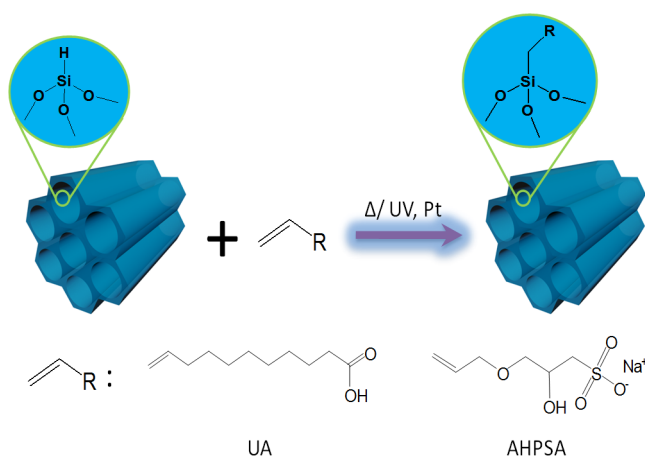
Received: September 9, 2013

Published: January 16, 2014

conventional postfunctionalization by organosilanes, the graft can be processed in the environment containing water, and the graft monomers or grafted chains will not easily block the pore channels because the hydrosilylation reaction usually will not produce no soluble composites like condensed organosilanes that can block the channels. Our method will not incorporate an excess Si–O layer but will rather link organic groups to pore walls by Si–C bonds directly, which are not sensitive to hydrolysis and oxidation reactions and have high survivability in strong acid, strong base, and even fluorination conditions.^{14b} The remnant abundant Si–H groups can also transfer to Si–Si bonds, which make the framework firmer.¹⁵ Second, the monomers for grafting are very abundant, allowing us to acquire various kinds of surface-functionalized PMSs. Especially, long-chain molecules and polymers can be grafted without destruction of the ordered mesoporous structures. Third, the modified functional groups are not limited, compared with the method of “co-condensation”. Moreover, the terminal trialkoxyorganosilanes for “grafting” or “co-condensation” are usually synthesized by terminal unsaturated compounds and the precursor for meso-HSiO_{1.5}, triethoxysilane. So the template-synthesized meso-HSiO_{1.5} provides another, more flexible way to access functional-groups-loaded PMSs with adjustable microstructures.

The surface organic functionalization of meso-HSiO_{1.5} was demonstrated by thermo- or UV-initiated hydrosilylation with two unsaturated compounds, undecylenic acid (UA) and 3-allyloxy-2-hydroxy-1-propanesulfonic acid sodium salt (AHPSA), respectively (Scheme 1). Similar to that using porous silicon, the process of surface modification by hydrosilylation has high graft efficiency, homogeneous dispersion, and high stability of organic groups. Especially, pore blocking is avoided because the unreacted monomer or

Scheme 1. Thermo/UV-Initiated Surface Organic Functionalization of meso-HSiO_{1.5} by Undecylenic Acid (UA) and 3-Allyloxy-2-hydroxy-1-propanesulfonic Acid Sodium Salt (AHPSA)



soft self-polymerized monomers do not form insoluble matter and can be easily washed away.

The compositions of the modified meso-HSiO_{1.5} were first confirmed by ²⁹Si and ¹³C CP MAS NMR spectroscopy, which give directly evidence for the successful graft. In ²⁹Si HPDEC NMR spectra (Figure 1a), the ungrafted meso-HSiO_{1.5} displayed two main signals at –75.4 and –85.7 ppm, which

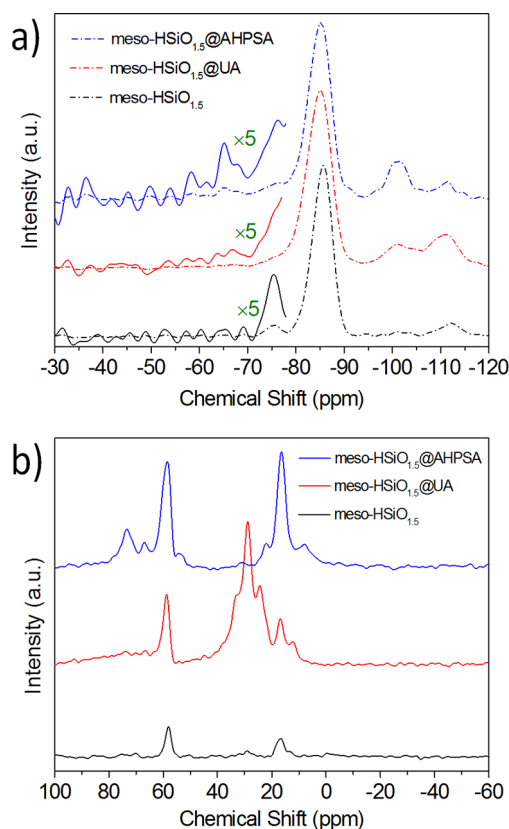


Figure 1. (a) ²⁹Si HPDEC and (b) ¹³C CP MAS NMR spectra of the modified meso-HSiO_{1.5}.

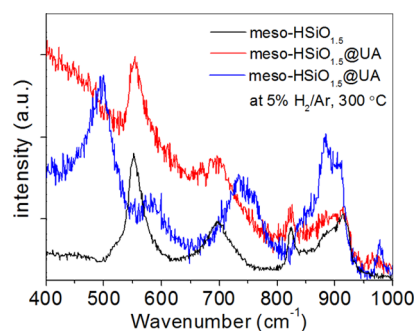


Figure 2. Raman spectra of meso-HSiO_{1.5}, meso-HSiO_{1.5}@UA, and meso-HSiO_{1.5}@UA heated at 300 °C under a slightly reducing atmosphere (5% H₂/95% Ar).

were assigned to T2 [H–SiO₂(OH)] and T3 (H–SiO₃) sites, respectively.¹² Small amounts of Q3 (HO–SiO₃) and Q4 (SiO₄) sites at –101.7 and –111.7 ppm, respectively, were also observed and were due to the hydrolysis of a small amount of Si–H sites (<10%). Upon hydrosilylation reaction with UA, the bulges that emerged around –58.0 and –65.2 ppm were assigned to T2 [CSi(OSi)₂(OH)] and T3 [CSi(OSi)₃] sites, respectively,¹⁶ confirming the modification by UA on the surface of meso-HSiO_{1.5}. For the sample reacted with AHPSA, clearly emerged peaks at –58.3 and –65.0 ppm gave similar proof for the grafting of AHPSA. These successful surface hydrosilylation reactions were also supported by the ¹³C CP MAS NMR spectra (Figure 1b). In ¹³C CP MAS NMR spectra, the curve of ungrafted meso-HSiO_{1.5} showed very little residual carbon, with the resonances at 16.7 and 58.0 ppm from unhydrolyzed Si–OEt groups, residual surfactant, or ethanol.¹⁷

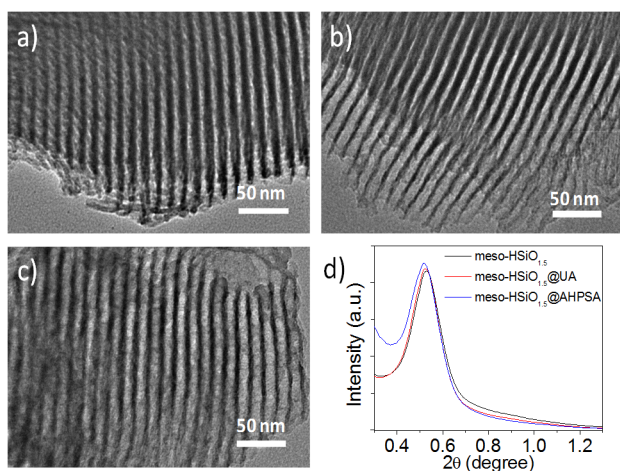


Figure 3. TEM images of (a) meso-HSiO_{1.5}, (b) meso-HSiO_{1.5}@UA, (c) meso-HSiO_{1.5}@AHPSA, and (d) SAXS curves of the three samples.

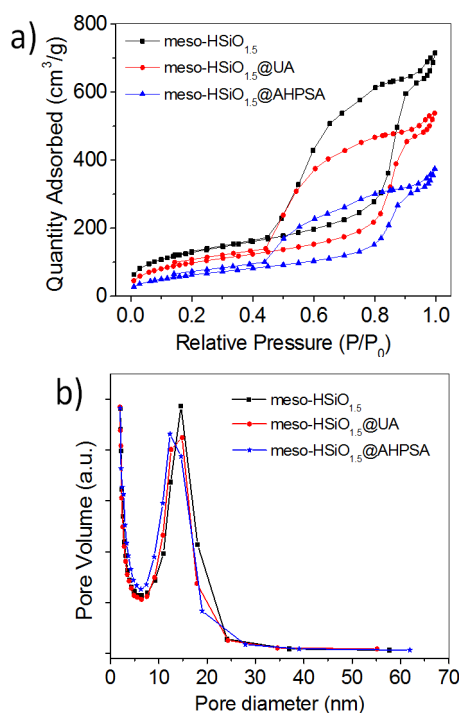


Figure 4. (a) N₂ adsorption/desorption isotherms and (b) pore size distribution of meso-HSiO_{1.5}, meso-HSiO_{1.5}@UA, and meso-HSiO_{1.5}@AHPSA.

Upon hydrosilylation, the spectra clearly showed that alkyl groups were incorporated intact in the channel wall. In the spectrum of the meso-HSiO_{1.5}@UA, the carbon attached to silicon resonated at 12.2 ppm, the carbon attached to carboxyl was observed at 37.9 ppm, and other alkyl carbons were

observed at 24.4, 28.9, and 33.1 ppm. For meso-HSiO_{1.5}@AHPSA, the spectrum showed a resonant peak of the carbon attached to silicon at 7.9 ppm and peaks at 22.1, 31.0, 66.9, and 73.4 ppm attributed to the resonance of alkyl carbons attached to oxygen, sulfur, and other alkyl carbons.

The FTIR spectra (Figure S1) also gave valuable information about the process. Before grafting, the FTIR spectrum showed a sharp Si–H stretching vibration at ~2255 cm⁻¹, an intense Si–O–Si vibration at 1000–1300 cm⁻¹, and an H–Si–O hybrid vibration at 800–900 cm⁻¹, consistent with an empirical composition of HSiO_{1.5}. The relatively broad peak at ~3500 cm⁻¹ is attributed to Si–OH groups, originating from hydrolyzed Si–OEt groups and limited hydrolysis of Si–H bonds. After hydrosilylation, the FTIR spectra exhibited clear alkyl stretching features at ~2900 cm⁻¹ (–CH₂ stretching) and at ~1460 and 1380 cm⁻¹ (–CH₂ and –CH deformation), consistent with alkyl groups of UA or AHPSA, which were almost invisible in the spectrum of the ungrafted sample. This gave indirect evidence for surface hydrosilylation. But the Si–C stretching band, which would directly confirm surface hydrosilylation, was obscured in the fingerprint region. The absorption peaks attributed to Si–H vibration did not present a remarkable decline because most Si–H bonds were preserved in the pore wall.

The quantitative result of atomic concentrations given by XPS is shown in Table S1. The increased content of carbon for modified samples and new evidence of sulfur and sodium elements confirmed the elemental composition of modified compounds. Thermogravimetric analysis (TGA, Figure S2) confirmed the content of grafted organic groups. For the sample of meso-HSiO_{1.5}@UA, the declining weight loss curve showed a slight grade before 300 °C, caused by loss of adsorbed H₂O or ethanol, and a steady level after 550 °C. In this region, a rapid drop of the curve was caused by decomposition of grafted organic groups, indicating its content to be ~9 wt%. Similarly, the curve for meso-HSiO_{1.5}@AHPSA showed a slight grades before 300 °C and a steady level after 600 °C, giving the content of grafted organic groups ~10 wt%. The TGA curves also indicated that the grafted samples were stable before 300 °C at inert atmosphere.

As mentioned above, the grafted composites still contained lots of Si–H groups in the pore walls, which could further transfer to Si–Si bonds and make the framework firmer. The formation of Si–Si bonds was observed by Raman spectroscopy. As shown in Figure 2, before thermal treatment, both meso-HSiO_{1.5} and meso-HSiO_{1.5}@UA have broad peaks centered at ~554 and 700 cm⁻¹, attributed to Si–O–Si bending and likely symmetric H–Si–O wagging modes, respectively. After thermal treatment of meso-HSiO_{1.5}@UA in a slightly reducing atmosphere (5% H₂/95% Ar), a broad peak centered at ~498 cm⁻¹ arose, which was characteristic of Si–Si.

On the basis of successful surface graft, a further question regards the structural information on the grafted meso-HSiO_{1.5}. Representative transmission electron microscopy (TEM)

Table 1. Surface Area, Pore Volume, Pore Diameter, *d*-Spacing, and Wall Thickness of meso-HSiO_{1.5}, meso-HSiO_{1.5}@UA, and meso-HSiO_{1.5}@AHPSA

sample	surface area (m ² /g)	pore volume (cm ³ /g)	pore diameter (nm)	<i>d</i> ₍₁₀₀₎ (nm)	wall thickness (nm)
meso-HSiO _{1.5}	472	1.13	14.5	16.7	6.0
meso-HSiO _{1.5} @UA	364	0.85	13.8	17.0	7.0
meso-HSiO _{1.5} @AHPSA	236	0.59	13.0	17.2	8.1

images and small-angle X-ray scattering (SAXS) curves of the resultant samples are shown in Figure 3. In Figure 3a, the TEM image shows the periodic parallel alignment of mesoporous channels in meso-HSiO_{1.5}, which gave a pore–pore distance of ~14 nm, a pore diameter of ~8 nm, and a wall thickness of ~6 nm. After grafting with UA or AHPSA, both meso-HSiO_{1.5}@UA and meso-HSiO_{1.5}@AHPSA kept the ordered mesoporous structure with enlarged pore–pore distance of ~15 nm but without obvious destruction of periodic parallel channels, as shown in Figure 3b,c, respectively. The long-range ordering of the mesoporous structure was also verified by SAXS (Figure 3d). The intense (100) diffraction peaks indicated the regular arrangement of 2D hexagonal mesopores, not only in meso-HSiO_{1.5} but also in grafted meso-HSiO_{1.5}@UA and meso-HSiO_{1.5}@AHPSA. The peak of grafted samples shifted left, which corresponds to the expansion of pore–pore distance.

Additionally, N₂ sorption data give clear evidence of the mesoporosity of the ungrafted meso-HSiO_{1.5} and grafted meso-HSiO_{1.5}@UA and meso-HSiO_{1.5}@AHPSA (Figure 4). The adsorption/desorption branches of all samples displayed type IV isotherms typical for mesoporous materials. The N₂ sorption data also agreed with the TEM images and indicated that the sample contains ordered, uniformly sized cylindrical pores. Figure 4b shows a narrow mesopore size distribution of ~15 nm and abundant micropores, and the mesopore size decreased after surface grafting. Compared to meso-HSiO_{1.5}, the BET surface areas of meso-HSiO_{1.5}@UA and meso-HSiO_{1.5}@AHPSA decreased from 472 m²/g to 364 and 236 m²/g, respectively (Table 1). At the same time, the pore volume also decreased due to shrinking of the pore diameter. Together with the unit cell parameter obtained from the SAXS pattern and the data obtained from BET measurements, the walls were estimated to show a thickening of ~1–2 nm after grafting, in agreement with the incorporation of organic layers on the pore surface and proving the success of the grafting process.

In summary, a new strategy for organic functionalization of PMSs is demonstrated by hydrosilylation of the recently discovered “impossible” periodic mesoporous hydridosilica, meso-HSiO_{1.5}. It not only provides a flexible method to access functional-groups-loaded PMSs with adjustable microstructures but also overcomes the disadvantages of present pathways for organic functionalization of PMSs, such as blocking of pore channels, limitation of modified functional groups, and destruction of the ordered mesoporous structures by soft organic groups. The new method and materials will have wider applications based on both the structure and surface superiorities.

■ ASSOCIATED CONTENT

■ Supporting Information

Synthesis, characterization details and atomic concentrations, FTIR spectra, and TGA curves of meso-HSiO_{1.5}, meso-HSiO_{1.5}@UA, and meso-HSiO_{1.5}@AHPSA. This material is available free of charge via the Internet at <http://pubs.acs.org>.

■ AUTHOR INFORMATION

Corresponding Authors

zyxie@seu.edu.cn

gu@seu.edu.cn

Notes

The authors declare no competing financial interest.

■ ACKNOWLEDGMENTS

This work was supported by the National Basic Research Program of China (Grant 2012CB933302), NSFC (Grant 51102043), the Program for Changjiang Scholars and Innovative Research Team in University (IRT1222), and 333 Talent Project Foundation of Jiangsu Province.

■ REFERENCES

- (1) (a) Li, Z.; Barnes, J. C.; Bosoy, A.; Stoddart, J. F.; Zink, J. I. *Chem. Soc. Rev.* **2012**, *41*, 2590. (b) Wan, Y.; Zhao, D. Y. *Chem. Rev.* **2007**, *107*, 2821. (c) Yang, J.; Shen, D.; Zhou, L.; Li, W.; Li, X.; Yao, C.; Wang, R.; El-Toni, A. M.; Zhang, F.; Zhao, D. *Chem. Mater.* **2013**, *25*, 3030. (d) Li, W.; Zhao, D. *Adv. Mater.* **2013**, *25*, 142. (e) Teng, Z.; Zheng, G.; Dou, Y.; Li, W.; Mou, C. Y.; Zhang, X.; Asiri, A. M.; Zhao, D. *Angew. Chem., Int. Ed.* **2012**, *51*, 2173.
- (2) (a) Wang, W. D.; Grozea, D.; Kohli, S.; Perovic, D. D.; Ozin, G. A. *ACS Nano* **2011**, *5*, 1267. (b) Mizoshita, N.; Tani, T.; Inagaki, S. *Adv. Funct. Mater.* **2011**, *21*, 3291. (c) Wang, Y.; Wang, K.; Zhao, J.; Liu, X.; Bu, J.; Yan, X.; Huang, R. J. *Am. Chem. Soc.* **2013**, *135*, 4799. (d) Asefa, T.; Tao, Z. *Can. J. Chem.* **2012**, *90*, 1015.
- (3) (a) Hatton, B.; Landskron, K.; Whitnall, W.; Perovic, D.; Ozin, G. A. *Acc. Chem. Res.* **2005**, *38*, 305. (b) Yang, P.; Gai, S.; Lin, J. *Chem. Soc. Rev.* **2012**, *41*, 3679. (c) Lim, M. H.; Blanford, C. F.; Stein, A. *Chem. Mater.* **1998**, *10*, 467. (d) Aznar, E.; Marcos, M. D.; Martinez-Manez, R.; Sancenon, F.; Soto, J.; Amoros, P.; Guillem, C. J. *Am. Chem. Soc.* **2009**, *131*, 6833. (e) Linares, N.; Serrano, E.; Rico, M.; Balu, A. M.; Losada, E.; Luque, R.; Garcia-Martinez, J. *Chem. Commun.* **2011**, *47*, 9024. (f) Tarn, D.; Ashley, C. E.; Xue, M.; Carnes, E. C.; Zink, J. I.; Brinker, C. J. *Acc. Chem. Res.* **2013**, *46*, 792.
- (4) Hoffmann, F.; Cornelius, M.; Morell, J.; Fröba, M. *Angew. Chem., Int. Ed.* **2006**, *45*, 3216.
- (5) Vathyam, R.; Wondimu, E.; Das, S.; Zhang, C.; Hayes, S.; Tao, Z.; Asefa, T. *J. Phys. Chem. C* **2011**, *115*, 13135.
- (6) Zheng, Q.; Zhu, Y.; Xu, J.; Cheng, Z.; Li, H.; Li, X. *J. Mater. Chem.* **2012**, *22*, 2263.
- (7) Zhou, Z.; Zhu, S.; Zhang, D. *J. Mater. Chem.* **2007**, *17*, 2428.
- (8) Balkenende, A. R.; de Theije, F. K.; Kriege, J. C. K. *Adv. Mater.* **2003**, *15*, 139.
- (9) Wang, W. D.; Lofgreen, J. E.; Ozin, G. A. *Small* **2010**, *6*, 2634.
- (10) Hunks, W. J.; Ozin, G. A. *J. Mater. Chem.* **2005**, *15*, 3716.
- (11) Lofgreen, J. E.; Moudrakovski, I. L.; Ozin, G. A. *ACS Nano* **2011**, *5*, 2277.
- (12) Xie, Z.; Henderson, E. J.; Dag, Ö.; Wang, W.; Lofgreen, J. E.; Kübel, C.; Scherer, T.; Brodersen, P. M.; Gu, Z.-Z.; Ozin, G. A. *J. Am. Chem. Soc.* **2011**, *133*, 5094.
- (13) Dag, O.; Henderson, E. J.; Wang, W. D.; Lofgreen, J. E.; Petrov, S.; Brodersen, P. M.; Ozin, G. A. *J. Am. Chem. Soc.* **2011**, *133*, 17454.
- (14) (a) Nakano, H.; Nakano, M.; Nakanishi, K.; Tanaka, D.; Sugiyama, Y.; Ikuno, T.; Okamoto, H.; Ohta, T. *J. Am. Chem. Soc.* **2012**, *134*, 5452. (b) Sieval, A. B.; Demirel, A. L.; Nissink, J. W. M.; Linford, M. R.; van der Maas, J. H.; de Jeu, W. H.; Zuilhof, H.; Sudhölter, E. J. R. *Langmuir* **1998**, *14*, 1759. (c) Strother, T.; Cai, W.; Zhao, X.; Hamers, R. J.; Smith, L. M. *J. Am. Chem. Soc.* **2000**, *122*, 1205. (d) Linford, M. R.; Fenter, P.; Eisenberger, P. M.; Chidsey, C. E. D. *J. Am. Chem. Soc.* **1995**, *117*, 3145.
- (15) Hessel, C. M.; Henderson, E. J.; Veinot, J. G. C. *Chem. Mater.* **2006**, *18*, 6139.
- (16) (a) Takafuji, M.; Azuma, N.; Miyamoto, K.; Maeda, S.; Ihara, H. *Langmuir* **2009**, *25*, 8428. (b) Radi, B.; Wellard, R. M.; George, G. A. *Macromolecules* **2010**, *43*, 9957.
- (17) Hunks, W. J.; Ozin, G. A. *Chem. Mater.* **2004**, *16*, 5465.